Exp Astron (2013) 35:489–506
DOI 10.1007/s10686-012-9319-9

ORIGINAL ARTICLE

Pointing of HAGAR telescope mirrors

K. S. Gothe · T. P. Prabhu · P. R. Vishwanath · B. S. Acharya · R. Srinivasan · V. R. Chitnis · P. U. Kamath · G. Srinivasulu · F. Saleem · P. M. M. Kemkar · P. K. Mahesh · F. Gabriel · J. Manoharan · N. Dorji · T. Dorjai · D. Angchuk · A. I. D'souza · S. K. Duhan · B. K. Nagesh · S. K. Rao · S. K. Sharma · B. B. Singh · P. V. Sudersanan · M. Tashi Thsering · S. S. Upadhya · G. C. Anupama · R. J. Britto · R. Cowsik · L. Saha · A. Shukla

Received: 9 July 2012 / Accepted: 19 September 2012 / Published online: 13 October 2012

Abstract An array of seven atmospheric Cherenkov telescopes was commissioned at a high altitude site in Hanle in the Ladakh region of the Himalayas. The array called HAGAR has been designed to observe celestial γ-rays of energy >100 GeV. Each telescope is altitude-azimuth mounted and carries seven parabolic mirrors whose optic axes are co-aligned with the telescope axis. The telescopes point and track a celestial source using a PC-based drive control system. Two important issues in positioning of each HAGAR telescope are pointing accuracy of telescope axis and co-alignment of mirrors' optic axes with the telescope axis. We have adopted a three pronged strategy to address these issues, namely use of pointing models to improve pointing accuracy of the telescopes, RA-DEC scan technique to measure the pointing offsets of the mirrors and mechanical fine-tuning of off-axis mirrors by sighting a distant stationary light source. This paper discusses our efforts in this regard as well as the current status of pointing and monitoring of HAGAR telescopes.

Keywords Telescope pointing · γ-ray astronomy · Pointing model · Atmospheric Cherenkov telescopes

K. S. Gothe (✉) · B. S. Acharya · V. R. Chitnis · N. Dorji · A. I. D'souza · S. K. Duhan · B. K. Nagesh · S. K. Rao · S. K. Sharma · B. B. Singh · P. V. Sudersanan · S. S. Upadhya
Tata Institute of Fundamental Research, Homi Bhabha Road, Colaba, Mumbai 400005, India
e-mail: kiran@tifr.res.in

T. P. Prabhu · P. R. Vishwanath · R. Srinivasan · P. U. Kamath · G. Srinivasulu · F. Saleem · P. M. M. Kemkar · P. K. Mahesh · F. Gabriel · J. Manoharan · T. Dorjai · D. Angchuk · M. Tashi Thsering · G. C. Anupama · R. Cowsik · A. Shukla
Indian Institute of Astrophysics, Sarjapur Road, 2nd Block, Koramangala, Bangalore 560034, India

R. J. Britto · L. Saha
Saha Institute of Nuclear Physics, 1/AF, Bidhannagar, Kolkata 700064, India

1 Introduction

An array of seven atmospheric Cherenkov telescopes, called High Altitude GAmma Ray (HAGAR) array has been commissioned at Hanle, Ladakh, India (78°58′35″ E, 32°46′46″ N, 4,270 masl). This array has been designed to detect celestial gamma rays of energy >100 GeV using the Atmospheric Cherenkov Technique. The secondary charged particles (mostly positrons and electrons) present in the electromagnetic cascade due to the interaction of primary gamma rays and cosmic rays in the atmosphere cause the emission of Cherenkov light as the cascade propagates down the atmosphere. Gamma rays have to be detected in the presence of copious amount of cosmic rays, which are isotropic in nature.

The Cherenkov light is beamed in the forward direction with an opening angle of about a degree in air. Therefore, by sampling the wavefront of Cherenkov light at different telescopes the direction of incoming shower can be estimated by triangulation. Figure 1 shows a typical distribution of the arrival direction of Cherenkov photons incident on an area of 0.65 m^2 (corresponding to one mirror) with respect to the direction of primary gamma rays as obtained from simulations. These simulation were performed using CORSIKA package [1, 2] for primary gamma ray energy of 200 GeV, incident vertically at a distance of 100 m from the telescope (i.e. at a core distance of 100 m). As regard to detection of photons in a telescope, the Cherenkov photons due to primary gamma rays have to compete with the light due to isotropic night sky background besides the Cherenkov photons due to cosmic rays. Both the cosmic ray background and night sky background could be reduced by restricting the telescope field of view to a few degrees while ensuring that the telescopes do not lose significantly Cherenkov photons due to primary gamma rays.

The telescopes have to be oriented to the source direction and track the object accurately as the Earth rotates. Our aim was to have a pointing and tracking accuracy of the order of magnitude required to capture as many

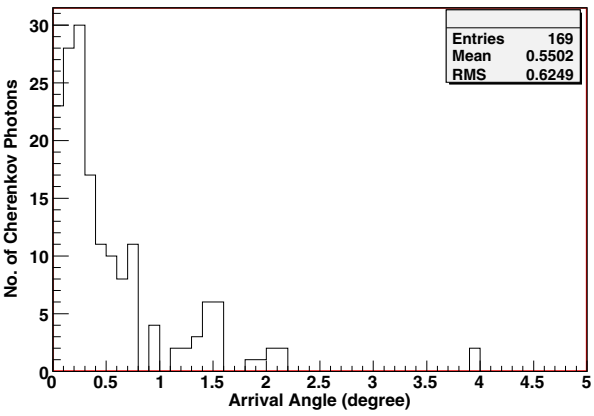

Fig. 1 A typical distribution of arrival direction of Cherenkov photons collected by one of the mirrors of HAGAR array. The arrival directions are given with respect to the primary gamma ray (mirror axis). The distribution was obtained through Monte Carlo simulation for a vertically incident primary γ-ray of 200 GeV energy at a distance of 100 m from the centre of the array

atmospheric Cherenkov photons (induced by incident gamma rays) as possible. It can be seen from a typical distribution of Cherenkov photon arrival direction shown in Fig. 1 that the HAGAR mirror may lose 6–12 % of the Cherenkov photons for a pointing error of 0.2°–0.6° (12–36 arcmin) given that the field of view of the mirror is ∼3° (see Section 2). The loss of Cherenkov photons on account of error in pointing would result in the reduction of signal strength which in turn could increase the energy threshold of incident gamma rays. The target for pointing accuracy was set at 0.2° (12 arcmin) for HAGAR telescopes after due consideration to the cost effective solution to the system design. The first part deals with the absolute pointing of the reference axis of a telescope and the other part with co-alignment of axes of all the optical components within a telescope with the telescope reference axis.

2 HAGAR telescope system

The seven telescopes in HAGAR array are arranged in the form of a regular hexagon with six telescopes at the vertices and one at the centre. A schematic diagram of the layout of the array is shown in Fig. 2. The installation of telescopes started in the year 2005 and was completed by September 2008. The photograph of a HAGAR telescope with the enlarged views of its relevant components are shown in Fig. 3. Each telescope is alt-azimuth mounted. It has seven parabolic mirrors, each of ∼90 cm diameter with unity f/d ratio mounted on a single platform. The mirrors are mounted with their optic axes perpendicular to the elevation axis so that they all point to the same region of the sky. These mirrors focus the incoming paraxial light onto a very fast UV sensitive photomultiplier tube (PMT) located at their respective foci (Fig. 3a and c). The specified diameter of photocathode of the PMT is 44 mm and the corresponding field of view is ∼3°.

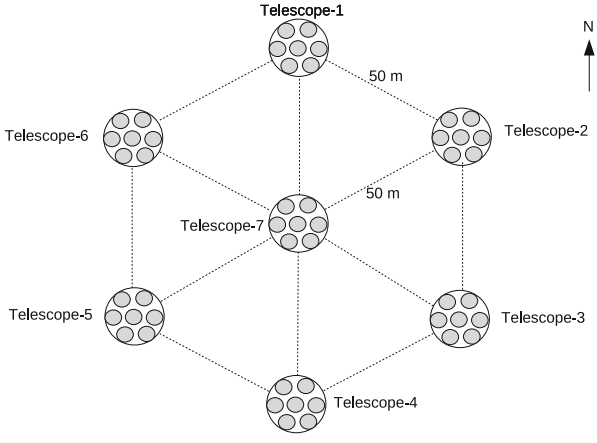

Fig. 2 Schematic diagram of HAGAR array of seven telescopes at Hanle (Ladakh, India)

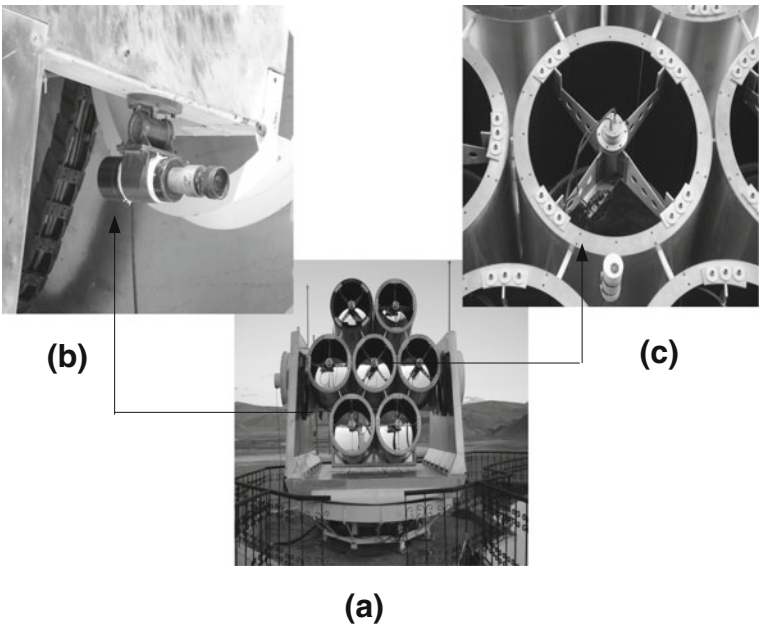

Fig. 3 Front view of one of the seven HAGAR telescopes with seven coaligned mirrors is shown in **a**. Also shown are the enlarged views of guide telescope with its mounting (**b**) and PMT (PHOTONIS XP2268B) with its shutter assembly (**c**)

A single control computer (Pentium PC) in the control room below telescope 7, provides user interface, computes the source position in real time and controls the motion of all seven telescopes under program control. The computer executes a control loop during which all seven telescopes are monitored and controlled independently of each other in a serial manner. The detailed discussion on the HAGAR telescopes servo system will be presented in the next paper which is under preparation. Mean tracking accuracy of the motion control servo is estimated to be about 16 arcsec. In the case of an ideal telescope this would define its tracking accuracy. A real telescope however, may not point exactly in the direction the servo moves it, and hence, through modeling, the command positions are determined such that the telescope will point at the desired direction when command coordinates are given instead of catalog positions.

3 Calibration of command position

HAGAR telescope control follows a sequence of transformations as shown in Fig. 4. It takes into account the correction required due to precession, rotation of the Earth and the physical misalignments in the telescope structure.

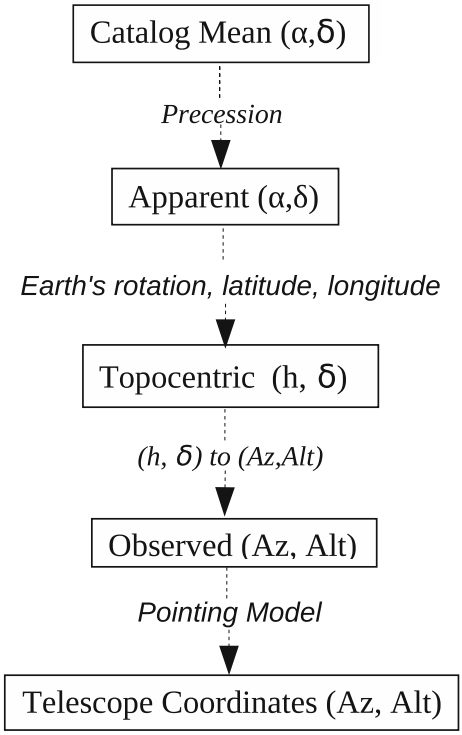

Fig. 4 Stages of transformations of catalog position of the source to telescope coordinates

The corrections required due to precession which is roughly 50 arcsec/year [3] is calculated and applied once for all at the beginning of the observation run. The maximum magnitudes of corrections due to nutation (∼17 arcsec), annual aberration (∼ 20 arcsec) [3] although significant, are currently not implemented.

3.1 Pointing model

A pointing model is needed to transform the star position as seen by the ideal telescope into the position seen by a real telescope. The model is a set of terms, each term being some function of a target position (azimuth and zenith distance) in the sky. The pointing model for HAGAR telescopes is a blend of analytical and empirical terms. The analytical terms attempt to provide pointing corrections based on possible physical misalignments and other mechanical distortions [4, 5]. These terms may also help to trace back to mechanical components of the telescope structure that cause the observed pointing errors. It should be noted that the f/d ratio being small, telescope structure is not so big and therefore structural rigidity could be ensured in the design of the HAGAR telescopes. The flexure of the mirror tubes in the

HAGAR telescopes were measured to be less than 0.06° at the zenith distance up to 80° confirming that the structure is rigid enough. These reasons prompted us not to go for finite element based computations of the telescope structure deformations. The pointing model for HAGAR is shown below:

Azimuth correction:

$$\Delta A = AN \times \sin A \times \tan E + AW \times \cos A \times \tan E + NPAE \times \tan E + IA + CA \times \sec E + ACEC \times \cos A + ACES \times \sin A \quad (1)$$

Zenith distance correction:

$$\Delta Z = -AN \times \cos A + AW \times \sin A + IE - CTS \times \sin E - CTT \times \tan E \quad (2)$$

where

A	Azimuth angle of the star;
E	Elevation angle of the star;
AN	Tilt of azimuth axis from vertical in North–South direction (due North is positive);
AW	Tilt of azimuth axis from vertical in East–West direction (due West is positive);
$NPAE$	Deviation in angle between the elevation axis and the azimuth axis from right angle;
IA	Zero error of azimuth encoder;
IE	Zero error of elevation encoder;
$ACEC$	Cosine component of once-per-revolution cyclic error in azimuth (this is due to mis-centered azimuth axis);
$ACES$	Sine component of once-per-revolution cyclic error in azimuth (this is due to mis-centered azimuth axis);
CA	Collimation error in azimuth (azimuth component of deviation angle between the elevation axis and the mean optic axis of seven mirrors from right angle); and
CTS and CTT	are empirically found coefficients.

The model implemented for each of the seven telescopes is the same. But the values of the coefficients in the model are different for each telescope. It should be noted that pointing model coefficients are worked out based on the pointing deviations of bright stars with respect to the telescopes. Zenithal component of these deviations include the contributions from the atmospheric refractions of the star light besides the contributions from the telescope misalignments and mechanical distortions. The value of refraction at HAGAR observation site computed using the equations by Eisele and Shannon (see reference [3]) is $\sim$ 1.0 arcmin for source zenith distances up to 60° [3]. As the refraction correction is not explicitly modelled in the pointing model it will lead to some error (<1 arcmin for zenith distance up to 60°) when the model is employed

to point to a star. In case of a gamma ray source the refraction of Cherenkov photons emitted in the atmosphere is much smaller than that of a star light seen from the same direction [6]. The resulting pointing error in zenith distance would be around 1 arcmin (0.02°) for the zenith distance up to 60°.

3.2 Pointing data collection

The data needed to determine the coefficients in the pointing model were obtained by taking pointing runs on suitable bright stars. The data consist of a series of pointing error measurements while attempting to point the telescopes to the bright stars. To facilitate easy readout of telescope pointing errors, a small guide telescope (Fig. 3b) is fitted onto the elevation shaft of each telescope. The pointing direction of the guide telescope is considered as reference axis of the telescope. The telescope is aligned to the selected bright star and tracked under computer control using the raw encoder values and the source coordinates reduced to observed coordinates as seen by an ideal telescope.

The guide telescope is fitted with a CCD camera (ST-4) to make precise pointing error measurements. After the telescope starts tracking the chosen star, its image is brought to the center of the CCD field of view by giving offsets in azimuth and elevation using control program itself. The pixel size of the CCD mounted onto the guide telescope is ∼20 arcsec and therefore the accuracy with which the star image is centered in the field of view is ±10 arcsec. Once the image is centered, the azimuth and elevation angles of the star along with the offsets in azimuth and elevations were recorded. The exercise was repeated for many stars or the same stars at different hour angles.

3.3 Pointing model results

We present here the results of analysis of the pointing run data collected in the year 2009. For each telescope the data were obtained for ∼20 bright stars in a single night. The ranges of zenith distance of the stars chosen for the runs were 19–82°, 8–80°, 5–80°, 8–80°, 6–75°, 4–79°, 9–80° for telescopes 1–7, respectively.

For each star observed by a guide telescope, the absolute value of the pointing offset as well as the position of the image of the star in the focal plane of the guide telescope was determined by taking into account the corresponding observed offsets in azimuth and elevation. The diagram to the left in Fig. 5 shows the observed positions of stars with respect to the guide telescope axes in the form of gnomonic projections. The mean and standard deviation for the distribution of the absolute pointing errors were computed for each of the telescopes and are given in column 2 of Table 1. The contribution to the large pointing errors could be due to collimation errors between the guide telescopes and the mounts, zero errors of the encoders and the imperfections in the telescopes structures and indeed one needs pointing model for orienting the telescopes to correct directions.

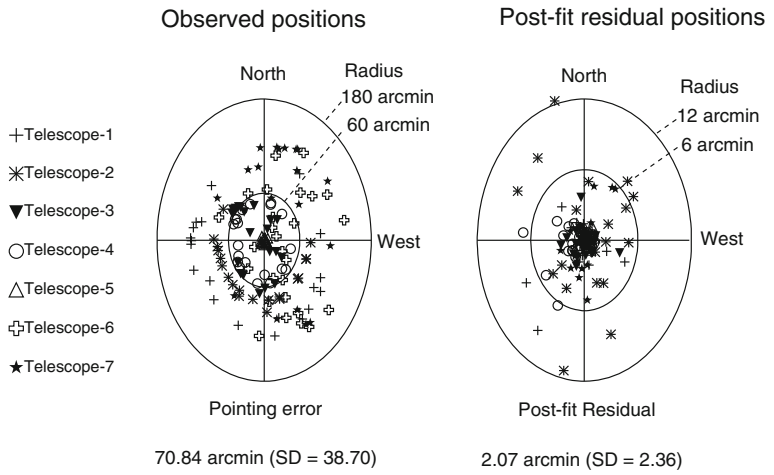

Fig. 5 Scatter diagram of pointing data of bright stars observed by guide telescopes (*left*) and that of post-fit pointing data after applying pointing model corrections to the observed data (*right*). The *centre* of the circles represents the pointing direction of guide telescope and the distribution of the stars positions for different telescopes is shown as dots with different symbols. Note the difference in scales of the figures

The coefficients in the pointing model were estimated using weighted least-squares technique [3, 7]. The values are shown in Table 2a and b. It is to be noted that while the observations with guide telescope provide good estimates of the coefficients related to the mechanical mount, they have no information on the collimation error between the optical axes of the mirrors on the mount and the guide telescope. Hence the term 'CA*sec(E)' is not included at this stage while estimating the coefficients in the pointing models described by (1). This term is introduced at a later stage (Section 4) after determining mean pointing direction of the seven mirrors in each telescope (see Section 4.4.2).

The derived coefficients are given in Table 2a and b. The diagram to the right in Fig. 5 shows gnomonic projections of the post-fit positions of the stars after subtracting pointing model corrections from observed errors. The

Table 1 Observed and post-fit absolute pointing errors on the sky based on the pointing runs taken in the year 2009

Telescope number	Observed pointing error (arcmin)	Post-fit error after subtracting pointing model correction from observed error (arcmin)
1	113.41 (SD = 8.67)	2.24 (SD = 2.35)
2	78.55 (SD = 4.08)	5.44 (SD = 3.11)
3	47.89 (SD = 17.21)	1.47 (SD = 0.99)
4	50.01 (SD = 4.45)	2.06 (SD = 1.91)
5	4.24 (SD = 2.00)	0.63 (SD = 0.37)
6	80.39 (SD = 39.29)	0.52 (SD = 0.30)
7	107.75 (SD = 20.95)	2.42 (SD = 1.64)

Table 2 The estimates of the coefficients in the pointing model based on the pointing runs taken in the year 2009

(a)

Telescope number	CTT (arcsec)	CTS (arcsec)	IE (arcsec)	IA (arcsec)
1	334.6 ± 22.3	1110.7 ± 55.1	6974.8 ± 16.8	−2304.5 ± 76.3
2	0.38 ± 13.6	16.4 ± 167	4611.2 ± 104.8	1577.4 ± 44.9
3	42.0 ± 7.8	603.5 ± 39.0	1890.0 ± 19.6	−4141.6 ± 14.5
4	−8.84 ± 4.7	−43.1 ± 44.6	2085.6 ± 26.2	−2017.1 ± 46.9
5	−22.7 ± 1.3	69.2 ± 13.3	−81.1 ± 9.8	60.2 ± 6.0
6	1.0 ± 0.3	−504.3 ± 11.0	−283.1 ± 8.7	8405.6 ± 4.1
7	35.1 ± 4.0	−159.4 ± 80.1	−745.6 ± 55.5	7137.7 ± 36.3

(b)

Telescope number	AN (arcsec)	AW (arcsec)	NPAE (arcsec)	ACEC (arcsec)	ACES (arcsec)
1	−104.1 ± 6.1	293.0 ± 10.1	−2057.0 ± 54.1	−81.5 ± 52.3	−56.1 ± 52.6
2	307.4 ± 47.7	312.6 ± 47.6	−2537.6 ± 60.8	−438.6 ± 38.4	−344.9 ± 41.8
3	155.3 ± 12.3	−94.2 ± 9.4	654.2 ± 9.8	25.7 ± 13.0	106.3 ± 11.2
4	−166.0 ± 10.2	−35.5 ± 21.0	−890.7 ± 22.4	−82.3 ± 47.7	−1.5 ± 24.8
5	238.4 ± 4.7	63.2 ± 5.3	202.8 ± 6.7	−51.2 ± 6.8	−106.6 ± 8.8
6	−131.4 ± 1.0	35.8 ± 1.0	589.9 ± 1.0	−32.1 ± 5.2	96.1 ± 4.7
7	52.5 ± 22.5	−154.4 ± 22.1	2098.2 ± 27.4	150.4 ± 42.6	86.0 ± 39.8

post-fit residual for all telescopes together was computed to be 2.07 arcmin (SD = 2.36) or 0.0345° (SD = 0.0393). Similarly the post-fit residual was computed separately for each telescope and is given in column 3 of Table 1. A comparison of observed and post-fit error for each telescope as shown in column 2 and column 3 respectively of the Table 1 clearly indicates goodness of the fits of the pointing models.

3.4 Pointing model for zenithal region

Since the pointing data samples in the zenithal region were sparse, the model based on the data is valid only for non-zenithal positions. It can be seen from the pointing models (1) and (2) that the corrections show divergence in the zenithal region due to the elevation dependent terms.

As an alternative, we use a linear approximation in the zenithal region. The zenith distance corrections in the region $70° \leq E \leq 80°$ were computed using the terms "$-CTS \times \sin E - CTT \times \tan E$" alone in the pointing model (2). A linear fit "$m \times E + c$" was worked out on these computed values of corrections, where m and c are the fit parameters. To point and track the region $80° \leq E < 90°$ degree, the terms "$-CTS \times \sin E - CTT \times \tan E$" in the pointing model (2) are then replaced by the linear fit "$m \times E + c$".

For vertical pointing required for certain calibrations, a different algorithm is adopted. First, in a separate exercise the telescopes were made vertical manually by using a magnetic protractor with a measurement uncertainty of ±15 arcmin (±0.25°). The azimuth and elevation encoder values were noted

for the vertical position of the telescopes. In order to point the telescope in vertical direction, the control program uses these values as target readings.

4 Pointing of mirrors

The seven mirrors of each telescope are independently mounted on a single platform. It is necessary to ensure that the optic axes of these mirrors are aligned with each other and also with the guide telescope axis. This is achieved as follows.

4.1 Mirror co-alignment procedure

The co-alignment between the guide telescope and the seven mirrors is done manually by sighting a stationary distant light source. The light source is situated at a distance of ∼1 km at an elevation angle ∼10°. To align any given mirror, the photo-tube is replaced with a ground glass assembly at the focus. The mounting of the assembly is such that the glass sits at the same position as the cathode of the photo-tube and one can see the image of the light source directly onto the glass. The centering of the image is achieved by using three tip-tilt screws provided on the back of the mirror cell. Cross wire markings made on the ground glass help to judge the centroid of the image.

4.2 Accuracy in mirror co-alignment

In general, the pointing error of a mirror in a telescope has following three components:

1. The component due to the pointing error of the guide telescope itself;
2. An offset of the mean pointing direction of seven mirrors with respect to the guide telescope axis;
3. An offset of the optic axis of the mirror with respect to the mean pointing direction.

The values of the former two components will be the same for all the seven mirrors in a telescope whereas the third component will differ from mirror to mirror. We have devised a method called RA-dec scan to estimate these components. The mean pointing error of the seven mirrors within a telescope as obtained in a RA-dec scan accounts for the first two components mentioned above and may be used to refine the pointing model for the telescope (i.e. pointing model may be updated to compensate for these errors). The deviation of a mirror's pointing error (obtained from the scan) from the mean pointing error would then account for the third component. The mirrors whose optic axes are off-set with respect to the mean pointing direction are re-aligned mechanically. This is a trial and error process.

4.3 Scan procedure

In a RA-dec scan, the region around the telescope pointing direction is scanned independently in RA and declination space for a maximal rate of PMTs pulses. At the beginning of each scan, the telescope control program acquires and tracks a bright star. Then a series of manual offsets in the star's RA coordinates are introduced while holding onto the star's declination (i.e. declination offset $= 0°$). At each step, the PMT pulse rates are recorded for a few seconds. Similarly, a series of manual offsets in declination coordinates are introduced while holding onto the RA coordinate of the star (i.e. RA offset $= 0°$) and the PMT pulse rates are recorded.

Figure 6 show typical PMT pulse rate profiles as a function of offset angle (i.e. PMT pulse rate *vs.* offset profiles) for a mirror in a telescope obtained from the scans. It is to be noted that the star image need not go through the center of field of view of PMT during these two independent scans. Nevertheless the central value of the profile gives the corresponding offset of the star in RA or declination, as the case may be, with respect to mirror axis. The negative of RA offset is the offset in hour angle of the star with respect to the mirror axis. The range of manually given RA offset over which the star remains in the field of view of a PMT during the RA scan increases with the declination (since the telescope moves along the RA small circle). To get a proper peaking of the rate then would require larger RA offset range to be covered for the RA scan which means larger will be the time span to perform the scan. For this reason, only a star with declination angle (δ) in the range $-30° < \delta < +40°$ is chosen for a scan to ensure that a position of the star does not change appreciably over the scan period and one can associate the observed offset of the star to a unique star position.

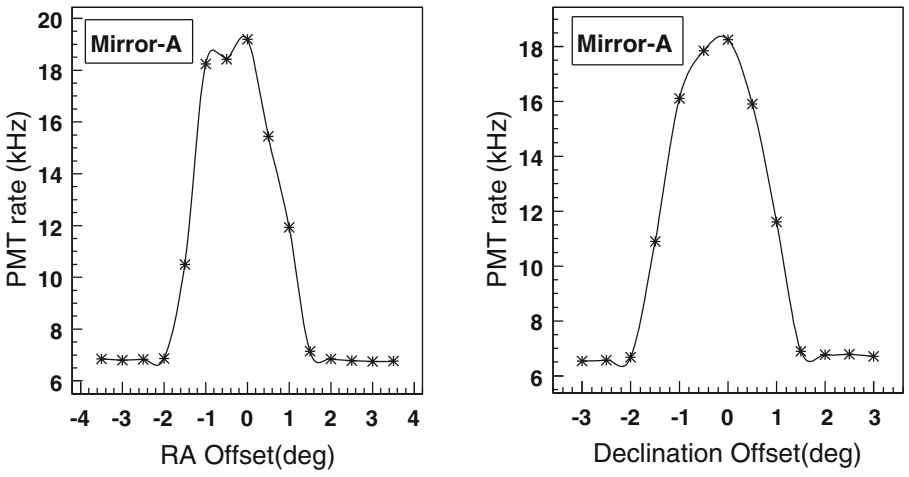

Fig. 6 Typical PMT rates profiles for a mirror in HAGAR telescope number 3 during RA-dec scan. The scan was taken on 25 August 2008 for star Markab (magnitude = 2.6)

4.4 Analysis of RA-Dec scans

After the stars' offsets with respect to the mirrors are determined, the absolute pointing error P of a mirror (error between the star and the pointing direction of a mirror) is computed using equation

$$P = \arccos\left((\sin(\delta) \times \sin(\delta_0) + \cos(\delta) \times \cos(\delta_0) \times \cos(h - h_0)\right) \tag{3}$$

where h, δ are respectively the hour angle and declination of the star, h_0, δ_0 are respectively the hour angle and declination of the mirror's optic axis.

4.4.1 Misalignment of the mirrors

The misalignment between the optic axis of a mirror and the pointing direction of the telescope (collimation error) may be decomposed into two components: collimation error in azimuth (CA_r) and zenith angle (CZ_r). These errors are computed in the following way. For each mirror in a telescope the observed offsets of a star in hour angle and declination with respect to the mirror $[\Delta h, (\delta - \delta_0)]$, are converted into the offset of the mirror in azimuth ($(\Delta A)_{\text{mir}}$) and zenith angle ($(\Delta Z)_{\text{mir}}$) with respect to the star. The mean values of the seven offsets in azimuth ($\overline{\Delta A}$) as well as in zenith angle ($\overline{\Delta Z}$) are then computed for the telescope. Thus $\overline{\Delta A}$ and $\overline{\Delta Z}$ are the offsets of the mean pointing direction of the mirrors with respect to the star. The offset of a mirror in azimuth (ΔA_r) and zenith angle (ΔZ_r) with respect to the mean pointing direction of the mirrors given by

$$\Delta Z_r = (\Delta Z)_{\text{mir}} - \overline{\Delta Z} \tag{4}$$

$$\Delta A_r = (\Delta A)_{\text{mir}} - \overline{\Delta A} \tag{5}$$

The collimation error in Azimuth (CA_r) is then derived from ΔA_r for individual mirrors by using following equation.

$$CA_r = \Delta A_r \times \cos(E) \tag{6}$$

where E is elevation angle of the star. The zenithal collimation error (CZ_r) of each mirror is ΔZ_r itself.

$$CZ_r = \Delta Z_r \tag{7}$$

Mean values of the collimation errors of a mirror over all the scans, namely $\overline{CA_r}$ and $\overline{CZ_r}$ are given by

$$\overline{CA_r} = (1/n) \times \sum CA_r \tag{8}$$

$$\overline{CZ_r} = (1/n) \times \sum CZ_r \tag{9}$$

where $n =$ number of the scans taken.

The mirrors that are having large mean values of the collimation errors need mechanical re-alignment. To do the re-alignment, first a reference mirror (whose pointing direction is estimated closest to mean pointing direction of all the mirrors in a telescope) is determined. Then the required mirrors are mechanically re-aligned with the reference mirror.

The rms values of collimation errors ($CA_{\rm rms}$, $CZ_{\rm rms}$) over all seven mirrors in a telescope and over all the scans are measures of the degree of misalignment of mirrors in the telescope.

4.4.2 Collimation error between guide telescope and mirrors

As pointed out earlier in Section 4.2, the origin of the mean offsets, namely $\overline{\Delta A}$ and $\overline{\Delta Z}$ is due to collimation error of the mean direction of seven mirrors in a telescope with respect to the guide telescope and may be taken care of by suitably modifying the pointing model itself as explained below.

(a) The mean value of offset $\overline{\Delta Z}$ averaged over all scans for each telescope may be algebraically added to the existing values of corresponding elevation encoder zero error i.e. IE in the pointing model.

(b) For each telescope, the data $\overline{\Delta A}$ vs sec(E) may be fitted to following equation:

$$\overline{\Delta A} = (CA)_m \times \sec(E) + (IA)_m \tag{10}$$

where, $(CA)_m$ and $(IA)_m$ are constants and E is elevation angle of the star. Here $(CA)_m$ represents collimation error between the mean

Table 3 The coefficients in the pointing models used for the scans taken in May 2010

(a)

Telescope number	CTT (arcsec)	CTS (arcsec)	IE (arcsec)	IA (arcsec)
1	274.4	1254.5	6566.8	−1404.4
2	21.1	−201.8	2817.8	3183.2
3	43.0	586.3	221.7	−2012.3
4	−4.4	−49.3	−137.6	−189.1
5	5.9	−352.4	−1528.9	−581.4
6	336.3	−1707.8	−373.2	7265.0
7	39.1	−220.6	−1541.4	6322.4

(b)

Telescope number	AN (arcsec)	AW (arcsec)	NPAE (arcsec)	ACEC (arcsec)	ACES (arcsec)
1	94.0	266.2	−2079.7	−82.2	44.7
2	350.7	369.8	−2592.0	−533.7	−345.1
3	137.4	−83.6	656.5	14.6	122.3
4	166.2	−88.4	−872.0	28.3	47.8
5	562.2	9.4	−763.6	−16.0	−92.0
6	118.5	−182.0	498.7	26.6	95.4
7	14.0	−172.1	2115.5	163.3	127.3

pointing direction of seven mirrors in a telescope and corresponding guide telescope.

(c) The new value of the azimuth encoder zero error (IA) in the pointing model is then equal to the algebraic addition of the value used in the existing pointing model and $(IA)_m$.

(d) The term corresponding to the collimation error $(CA)_m$ in the pointing model is $(CA)_m * \sec(E)$ as given in (1).

4.5 Results and discussions

With an initial co-alignment of mirrors done as explained in the Section 4.1 and the basic pointing models ((1) and (2)), worked out from the pointing run data collected in 2009, the telescopes have gone through a few 'observe and correct' cycles for improving pointing accuracy of the mirrors. Each cycle starts with a set of RA-dec scans followed by mechanical re-alignment of mirrors which were found considerably off in the scans and refinement of pointing model. We present here the results from the latest such cycle.

Seven scans were taken in May 2010 for all the seven telescopes based on the coefficients in the pointing model given in Table 3a and b. Figure 7 shows the stars (acquired by telescope control program before the scans) in the focal plane as seen by each of the 49 mirrors in HAGAR array. The corresponding

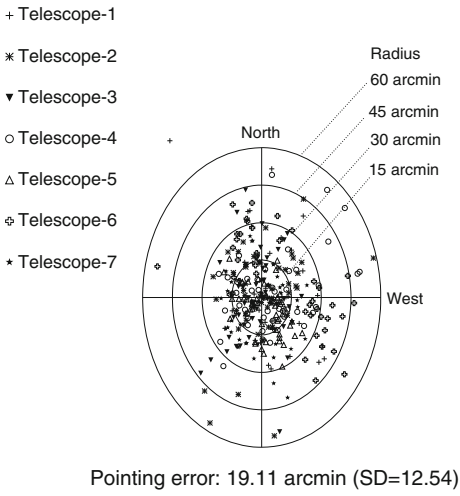

Fig. 7 Pointing offsets of all the 49 mirrors in HAGAR array inferred from the seven scans taken in May 2010. The azimuth and zenith distance of the stars chosen for the seven scans were (310.97°, 34.27°), (248.53°, 26.20°), (100.27°, 56.65°), (104.96°, 46.95°), (88.52°, 63.22°), (149.79°, 29.62°) and (253.75°, 47.81°). Pointing model for guide telescopes described in (1) and (2) without the CA term was used to point the telescopes to the stars. The *centre* of the concentric circles represents the focal point of each mirror and the *markers* represent the observed positions of the stars in the focal plane

Table 4 Estimated collimation errors of mirrors ($\overline{CA_r}$,$\overline{CZ_r}$) with respect to the mean pointing direction of seven mirrors in a telescope based on the scans in May 2010

Telescope number	Mirror-A (°)	Mirror-B (°)	Mirror-C (°)	Mirror-D (°)	Mirror-E (°)	Mirror-F (°)	Mirror-G (°)
1	0.25, −0.22	−0.04, −0.10	−0.02, −0.03	−0.46, 0.25	0.41, 0.23	0.23, 0.06	−0.24, −0.11
2	0.18, 0.14	−0.35, −0.59	−0.06, 0.25	−0.05, 0.01	0.12, −0.12	0.04, 0.32	0.13, −0.01
3	−0.17, −0.10	−0.17, −0.17	−0.14, −0.03	0.07, 0.00	0.40, 0.11	0.02, 0.16	−0.01, 0.03
4	0.12, −0.09	−0.21, 0.06	−0.14, −0.26	−0.12, 0.23	0.17, 0.16	0.23, 0.12	−0.05, −0.21
5	−0.09, 0.11	−0.03, −0.20	−0.17, −0.02	0.02, −0.02	0.02, −0.04	0.15, 0.12	0.10.0.05
6	0.19, −0.05	0.17, −0.02	−0.23, −0.15	−0.07, −0.07	−0.06, −0.03	−0.04, 0.28	0.09, 0.03
7	0.06, 0.00	−0.03, −0.08	−0.20, −0.13	0.12, 0.03	0.00, −0.15	0.02, 0.18	0.01, 0.15

Table 5 Coefficients of the terms in the pointing models used for the scans taken in September 2010

(a)

Telescope number	CTT (arcsec)	CTS (arcsec)	IE (arcsec)	IA (arcsec)	CA (arcsec)
1	274.4	1254.5	642.0	−215.0	1383.0
2	21.1	−201.8	2817.8	1111.0	1787.0
3	43.0	586.3	114.0	−2533.0	−456.4
4	−4.4	−49.3	438.0	−3474.0	2606.0
5	5.9	−352.4	−1601.0	824.0	−517.5
6	336.3	−1707.8	−1525.0	8084.0	684.3
7	39.1	−220.6	−1541.4	7966.0	−1762.0

(b)

Telescope number	AN (arcsec)	AW (arcsec)	NPAE (arcsec)	ACEC (arcsec)	ACES (arcsec)
1	94.0	266.2	−2079.7	−82.2	44.7
2	350.7	369.8	−2592.0	−533.7	−345.1
3	137.4	−83.6	656.5	14.6	122.3
4	166.2	−88.4	−872.0	28.3	47.8
5	562.2	9.4	763.6	−16.0	−92.0
6	375.6	−182.0	498.7	26.6	95.4
7	14.0	−172.07	2115.5	163.3	127.3

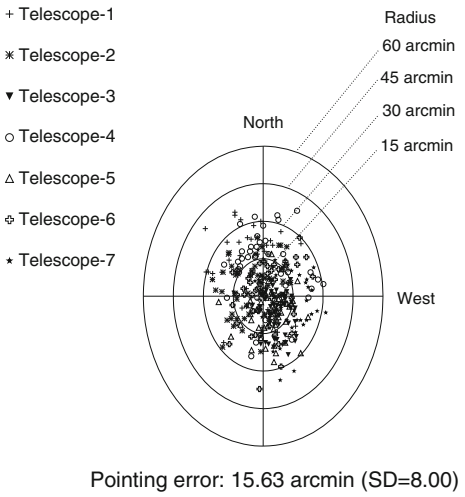

Fig. 8 Pointing offsets of all the 49 mirrors in HAGAR array inferred from the seven scans taken in September 2010. The azimuth and zenith distance of the stars chosen for the seven scans were (159.40°, 23.77°), (110.99°, 11.97°), (106.73°, 58.58°), (104.35°, 26.14°), (257.42°, 53.81°), (127.20°, 14.86°) and (277.11°, 42.12°). Pointing model for guide telescopes described in (1) and (2) was used to point the telescopes to the stars. The *centre* of the concentric circles represents the focal point of each mirror and the *markers* represent the observed positions of the stars in the focal plane

Table 6 RMS values of collimation errors ($CA_{\rm rms}$, $CZ_{\rm rms}$) between an individual mirror and the mean pointing direction in each telescope averaged over seven stars for which scans were taken

Telescope	Collimation errors ($CA_{\rm rms}$, $CZ_{\rm rms}$) in May 2010 (°)	Collimation errors ($CA_{\rm rms}$, $CZ_{\rm rms}$) in September 2010 (°)
1	0.29, 0.18	0.17, 0.16
2	0.18, 0.28	0.17, 0.14
3	0.19, 0.13	0.09, 0.07
4	0.20, 0.20	0.16, 0.14
5	0.11, 0.11	0.14, 0.13
6	0.15, 0.14	0.16, 0.11
7	0.13, 0.13	0.15, 0.14

average pointing error of HAGAR mirror was computed to be 19.11 arcmin (SD = 12.52 arcmin) or 0.3185° (SD = 0.2087).

Table 4 shows mean collimation errors ($\overline{CA_r}$,$\overline{CZ_r}$) of each mirror. Based on the values in Table 4, some of the mirrors which showed up large collimation errors, namely 1A, 1D, 1E, 1F, 2B, 3E, 4B, 4C and 4G were re-aligned. Also the fresh values for coefficients IE, IA and the newly introduced coefficient CA were worked out in a way explained in Section 4.4.2. Updated coefficients in the pointing model are shown in Table 5a and b.

With the updated pointing model, another set of scans was taken in September 2010. Figure 8 shows the corresponding results of these scans. Table 6 gives comparison between the rms values of collimation errors estimated from the scans taken in May 2010 and September 2010. It can be seen from the table that there is a noticeable improvement in co-alignments of the mirrors in telescopes 1–3. This may be attributed to the mechanical re-alignment of the mirrors. The pointing of mirrors/telescopes were improved further based on these scans. The estimate for overall pointing accuracy of a mirror in the HAGAR array was obtained and is 12.50 arcmin (SD = 6.95 arcmin) or 0.2083° (SD = 0.1158°) showing some improvement compared to the estimate from the scans taken in May 2010.

5 Conclusions and outlook

The accuracy of pointing and tracking of a telescope depends heavily on the accuracy of command positions corrected for imperfections in the telescope and its drive system which in turn are limited by the accuracy of pointing models (see Section 2). The post-fit pointing residual for the telescopes, as mentioned in Section 3.3 indicates that the telescope mounts are capable of pointing with 2 arcmin (0.03°) accuracy, but the current accuracy is limited by the mirror alignments to about 12 arcmin (0.2°). The RA-DEC scan technique provides a means of estimating the collimation error terms of the pointing model. The scan outputs can be used to figure out in a telescope, the off-axis mirrors to be re-aligned mechanically. Our next target would be to improve the pointing further below 12 arcmin (0.2°) by improving the co-alignments of the

mirrors in each telescope and also by improvising the mechanical arrangement for supporting the mirrors in the telescopes.

Acknowledgements We thank Prof. B. V. Sreekantan for his keen interest and encouragement. We also thank Dr. A. Krishnan for his guidance and helpful tips during the early stage of the telescope control system design. We thank Profs. P. N. Bhat, H. S. Mani, R. Koul and P. Bhattacharjee for their suggestions that helped reducing the pointing error. We thank the staff at Hanle for help with the operation of telescopes. Our thanks are due to IIA and TIFR staff members who have contributed at various stages of this project.

References

1. Knapp, J., Heck, D.: Extensive Air Shower Simulation with CORSIKA: A User's Guide, Version 6.7 (2007)
2. Heck, D., et al.: Forschungszentrum Karlsruhe Report, FZKA 6019 (1998)
3. Trueblood, M., Genet, R.: Microcomputer Control of Telescopes. Willman-Bell, Inc., USA (1985)
4. Wallace, P.T., Tritton, K.L.: Alignment, pointing accuracy and field rotation of the UK 1.2-m Schmidt telescope. Mon. Not. R. Astron. Soc. **189**, 115 (1979)
5. Wallace, P.T.: http://www.tpsoft.demon.co.uk/pointing.htm (1998–2010)
6. Bernlöhr, K.: Impact of atmospheric parameters on the atmospheric Cherenkov technique. Astropart. Phys. **12**, 255–268 (2000)
7. Gelb, A.: Applied Optimal Estimation. The MIT Press (1974)